

# A 3.4 – 6.2 GHz Continuously Tunable Electrostatic MEMS Resonator with Quality Factor of 460-530

Xiaoguang Liu<sup>†</sup>, Linda P.B. Katehi<sup>\*</sup>, William J. Chappell<sup>†</sup> and Dimitrios Peroulis<sup>†</sup>

<sup>†</sup>Birck Nanotechnology Center, School of Electrical and Computer Engineering, Purdue University, USA.

<sup>\*</sup>University of Illinois, Urbana-Champaign, USA.

liu79@purdue.edu, katehi@illinois.edu, dperouli@purdue.edu

**Abstract**—In this paper we present the first MEMS electrostatically-tunable loaded-cavity resonator that simultaneously achieves a very high continuous tuning range of 6.2 GHz:3.4 GHz (1.8:1) and quality factor of 460–530 in a volume of  $18 \times 30 \times 4 \text{ mm}^3$  including the actuation scheme and biasing lines. The operating principle relies on tuning the capacitance of the loaded-cavity by controlling the gap between an electrostatically-actuated membrane and the cavity post underneath it. Particular attention is paid on the fabrication of the tuning mechanism in order to avoid a) quality factor degradation due to the biasing lines and b) hysteresis and creep issues. A single-crystal silicon membrane coated with a thin gold layer is the key to the success of the design.

**Index Terms**—Evanescent-mode cavity, MEMS, quality factor, tuning, tunable filter, tunable resonator

## I. INTRODUCTION

There has been a growing interest in the use of evanescent mode cavity resonators to make low-loss, highly-selective preselect-filters for reconfigurable RF front-ends [1]-[2]. Compared to half-wave cavity resonators, evanescent mode resonators offer several advantages including substantially smaller volume [1]-[2] and larger spurious-free region [3] while maintaining a very high quality factor (Q) in the order of 500-1000. A capacitive post loaded evanescent mode resonator, shown in Fig. 1 offers the potential for high tunability due to the high sensitivity of the resonator frequency on the small gap between post top and the cavity ceiling. Several attempts have been made to create tunable evanescent mode resonators. The tuning mechanisms are primarily base on external piezoelectric actuators [4]-[5]. External piezoelectric tuning have achieved excellent RF performance but suffer from issues such as large overall volume, hysteresis, instability, and/or high power consumption. Electrostatic actuation, on the other hand, has been recognized for its merits of very low power consumption, fast actuation and no hysteresis in the analog actuation region. In this paper, we report the first electrostatically actuated MEMS tunable evanescent mode resonator that has a tuning range of 3.4 – 6.2 GHz (1.8:1) and Q of 460-530.

The success of the proposed resonator design relies partly on the use of Silicon-on-Insulator (SOI) wafers (Fig. 1) and on the biasing scheme. The device silicon layer is released to a movable diaphragm and a thin film Au is sputtered on it to

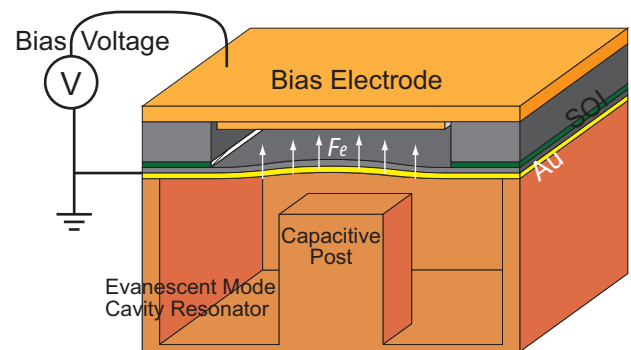


Fig. 1. Novel tunable evanescent mode resonator design using an electrostatically actuated thin diaphragm released from the single-crystal silicon device layer of an SOI wafer.

form the cavity ceiling. The resonant frequency is tuned by moving the diaphragm upwards after applying a dc voltage on a bias electrode placed above the diaphragm. Thus no biasing lines interfere with the RF fields. Furthermore, the nearly defect-free single-crystal silicon diaphragm provides a reliable and stable mechanical support. On the other hand, the highly conductive Au film ensures a high quality factor. The combination of the two offers a nearly ideal tuning scheme with no hysteresis and creep issues.

## II. DESIGN

### A. Frequency Tuning

The resonant characteristics of capacitive-post-loaded evanescent-mode cavity resonator are well-studied [2],[6]. The resonant frequency and quality factor are both functions of the cavity size, post size and the gap between the post top and cavity ceiling. The evanescent mode resonator is the cavity equivalent of a lumped element resonator and can be approximated by a lumped element L-C tank. The resonant frequency  $f_0$  is given by (1) in which  $C_{post}$  represents the capacitance between the post and cavity ceiling. [2]

$$f_0 \approx \frac{1}{2\pi \sqrt{L_0 (C_0 + C_{post})}} \quad (1)$$

Because the post top area  $A_{post}$  dimensions are far greater than the gap  $d$  (see Fig. 1),  $C_{post}$  can be approximated by the

parallel-plate capacitance formulae (2). Therefore, the resonant frequency's dependence on the gap  $d$  is given by (3)

$$C_{post} \approx \frac{\epsilon_0 A}{d} \quad (2)$$

$$f_0 \approx \frac{1}{2\pi\sqrt{L_0(C_0 + \epsilon_0 A/d)}} \quad (3)$$

Since  $C_0$  is typically very small compared to  $C_{post}$ , the resonant frequency  $f_0$  is approximately inversely proportional to the square root of the gap  $d$ . As a result, the frequency tuning range is dependent on the initial gap  $d_0$  and the maximum distance the diaphragm can deflect.

We use a simple 1-D spring-mass model to model the actuation of the diaphragm (Fig. 3). The relationship between the diaphragm's deflection  $x$  and bias voltage  $V$  for a circular diaphragm is given by (4), in which  $A$  is the area of the bias electrode,  $g_0$  the initial actuation gap (Fig. 3) and  $k$  the spring constant for the diaphragm [7].

$$\epsilon_0 \frac{AV^2}{2(g_0 - x)^2} = kx. \quad (4)$$

The analytical solution to (4) is

$$x = r_{real}(V, A, k, g_0) = \frac{1}{3}g_0 + \frac{K}{6k} + \frac{2g_0^3 k}{K}, \quad (5)$$

where

$$K = \sqrt[3]{k^2(-108\epsilon_0 AV^2 + 8g_0^3 k + 12VJ)}, \quad (6)$$

$$J = \sqrt{-3\epsilon_0 A(-27\epsilon_0 AV^2 + 4g_0^3 k)}. \quad (7)$$

The relationship between the resonant frequency  $f_0$  and  $V$  is then given by (8)

$$f_0 \approx \frac{1}{2\pi\sqrt{L_0(C_0 + \epsilon_0 A/d + r_{real}(V, A, k, g_0))}} \quad (8)$$

Since pull-in occurs at about  $g_0/3$  deflection, the maximum tuning range  $R_{max}$  is approximatively given by (9)

$$R_{max} \approx \sqrt{\frac{d_0 + g_0/3}{d_0}}. \quad (9)$$

In order to achieve a higher tuning range, a small  $d$  and a large  $g_0$  are desired. As shown in the next subsection though, careful balancing is needed between the desired tuning range and the required actuation voltage.

### B. Actuation Voltage

Although a larger  $g_0$  results in a higher tuning range, it also yields a higher actuation voltage. The actuation voltage is also dependent on the actuation area  $A$  and the spring constant  $k$ . While  $g_0$  is primarily determined by the tuning-range requirement,  $A$  can be chosen to reduce the actuation voltage by increasing the size of the bias electrode.

The spring constant of a circular diaphragm is given by (10)

TABLE I  
PARAMETERS FOR THE FINAL DESIGN

Capacitive Post Diamter	0.9 mm
Bias Electrode Size $A$	$5 \times 5 \text{ mm}^2$
Diaphragm Size	$7 \times 7 \text{ mm}^2$
Initial Capacitive Gap $d_0$	$5 \text{ }\mu\text{m}$
Initial Actuation Gap $g_0$	$45 \text{ }\mu\text{m}$
Residual Stress in Au $\sigma$	$30 \text{ MPa}$

$$k = k' + k'' = \frac{16\pi Et^3}{3R^2(1-\nu^2)} + 4\pi\sigma t, \quad (10)$$

where  $a$  and  $t$  are the diaphragm side length and thickness,  $E$  is the Young's modulus,  $\sigma$  the residual stress and  $\nu$  the Poisson's ratio [7]. In the presence of practical residual stress ( $>5 \text{ MPa}$ ), the  $k''$  term dominates the spring constant value particularly for large diaphragms with radius over 1 mm. Therefore, it is critical to achieve low residual stress in the sputtered Au film for low voltage operation.

The final design parameters are listed in Table. I. Ansoft HFSS [8] simulation results for resonant frequency and quality factor of the design is shown in Fig. 2. Fig. 3 shows the resonant frequency's dependence on the bias voltage based on the model derived in this section.

### C. Gold thickness impact on the $Q$

The gold skin depth is  $1.24 \text{ }\mu\text{m}$  at 4 GHz, assuming the conductivity of Au thin film is  $4.1 \times 10^7 \text{ Siemens/m}$ . The deposited Au film on the diaphragm is only  $0.5 \text{ }\mu\text{m}$ . The thickness of the Au film is primarily determined by pull-in voltage considerations and by the desire to keep the single-crystal SOI thickness much greater than the gold thickness. The penalty paid is a slightly reduced quality factor by approximately 200–300 as shown in Fig. 2.

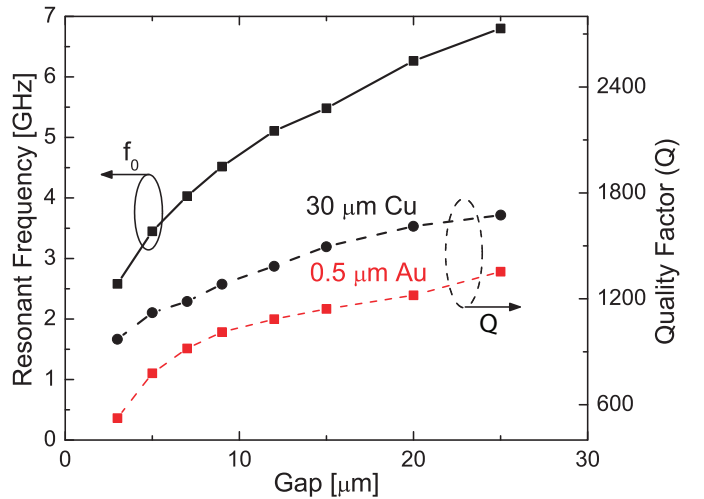


Fig. 2. Simulated resonant frequency and quality factor for the designed resonator.

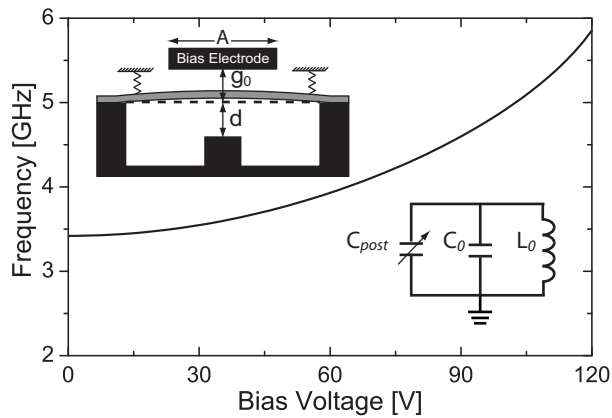


Fig. 3. Modelled resonant frequency dependence on the biasing voltage for the tunable resonator.

### III. FABRICATION

The fabrication process of the tunable resonator involves standard microfabrication steps and conventional machining techniques. It consists of three parts: a) the SOI diaphragm piece, b) the bias electrode piece, and c) the cavity piece. Fig. 4 summarizes the fabrication process flow.

The fabrication of the SOI piece starts with patterning an AZ9260 photoresist layer on the handle layer side as an etching mask for deep reactive ion etching (DRIE). The buried oxide layer has very high selectivity ( $> 200 : 1$ ) to silicon in the DRIE process and serves as an etch stop. After etching through the handle layer by DRIE, the oxide is removed by diluted HF solution. The device silicon layer is released upon the removal of the oxide layer. The released diaphragm is nearly perfectly flat due to the extremely low residual stress in the device layer. A  $0.5 \mu\text{m}$  thick Au layer is then sputtered on top of the released silicon diaphragm. The sputtering condition is carefully controlled to achieve a low tensile stress in the metal layer.

The bias electrode consists of two pieces of silicon bonded together. The thickness of the smaller piece  $h$  is controlled by wet etching in a 25% TMAH solution at  $80^\circ\text{C}$ . The etching condition ensures  $< 0.1 \mu\text{m}$  thickness control and a very smooth surface finish. The two pieces are then metalized with Au on both sides and bonded together by Au-Au thermal-compression bonding at  $350^\circ\text{C}$  and 50 MPa pressure. A layer of  $2 \mu\text{m}$  Parylene-C is deposited on the smaller piece side to create an insulation layer for biasing.

The cavity with the evanescent mode post is machined from a Rogers TMM substrate. The process starts with drilling vias that form the boundary of the resonant cavity and the feeding coplanar waveguide structure. The vias are electroplated with copper. Then a milling-machine is used to create the evanescent post by removing the substrate material around it. The removal of the substrate material also helps to increase the quality factor of the resonator by reducing dielectric loss. The vias and the post are then metalized by electroplating a thick layer of copper. The top copper layer of the cavity and the

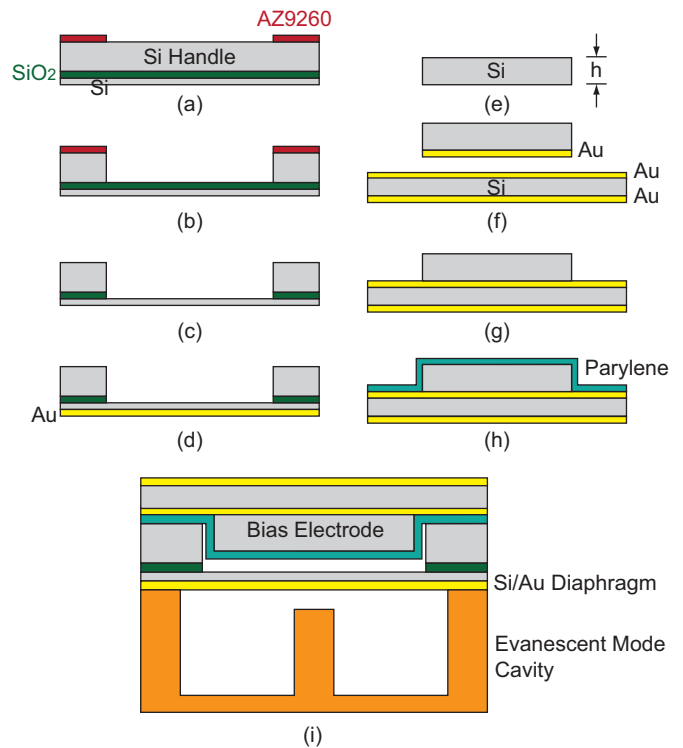


Fig. 4. Fabrication process for tunable evanescent mode resonator. (a) AZ9260 patterning; (b) DRIE; (c) Oxide etch; (d) Au sputter; (e) TMAH etch; (f) Au sputter; (g) Au-Au bonding; (h) Parylene deposition; (i) Tunable resonator assembly.

evanescent post is polished to reduce the surface roughness.

The SOI diaphragm piece is attached to the cavity by silver epoxy cured for 20 min at  $125^\circ\text{C}$ . The bias electrode is fixed on the SOI diaphragm by non-conductive epoxy cured at room temperature. After the assembly is done, two SMA connectors are soldered to both ends of the resonator to characterize the RF performance.

Fig. 5 shows the fabricated devices.

### IV. MEASUREMENTS AND DISCUSSION

The RF measurements are taken with an Agilent 8722ES network analyzer. Fig. 5(b) shows the measurement setup.

Fig. 6 shows the measured weak-coupled transmission of the tunable resonator under several biasing voltages. The resonator shows a total tuning range from 3.42–6.16 GHz under a bias voltage of 0–130 V. At 130 V, the movable diaphragm is pulled in to the top bias electrode. Fig. 7 (a) shows the resonant frequency change under 0–120 V bias voltage. Although we approximated the spring constant of the square diaphragm by that of a circular diaphragm, our model shows very good agreement with experiment results.

The measured quality factor of the tunable resonator at each resonant frequency is shown in Fig. 7 (b) and compared to the HFSS simulation result. The measured quality factor is 40% smaller than the simulated values and is less frequency dependent. This suggests that the loss in quality factor is primarily attributed to the low conductivity in the cured silver

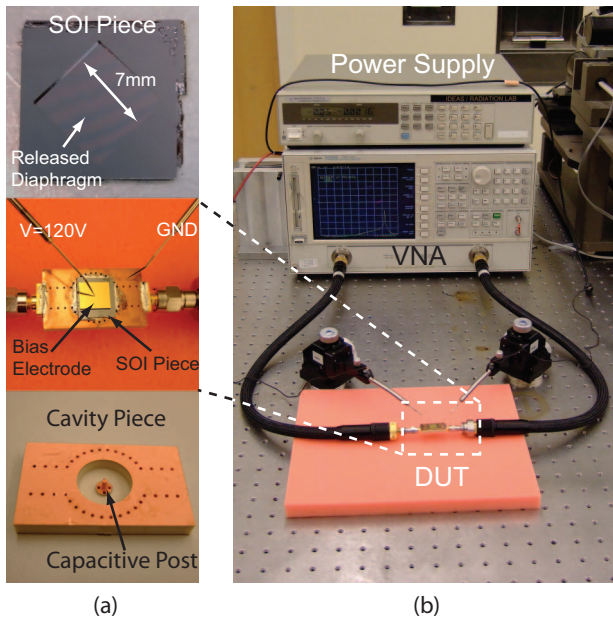


Fig. 5. Pictures of, (a) the fabricated parts; (b) measurement Setup.

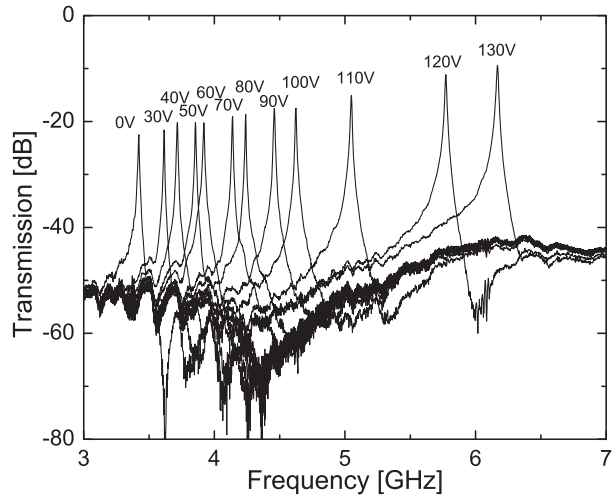


Fig. 6. Measured transmission of the tunable evanescent mode resonator at different biasing voltages.

epoxy that connects the movable diaphragm to the bottom cavity.

## V. CONCLUSION

A new electrostatically-tunable MEMS cavity resonator is demonstrated in this paper. A very high quality factor of 460-530 is maintained through a continuous tuning range of 3.4–6.2 GHz (1.8:1). The required electrostatic voltage ranges from 0–130 V. Special attention is paid on the biasing scheme and the fabrication process to ensure a robust mechanical structure that preserves the high quality factor of the cavity. The primary material of the tuning membrane is single-crystal silicon that is coated with a thin gold layer. Such resonators are key building blocks of pre-select filters in reconfigurable RF front-ends.

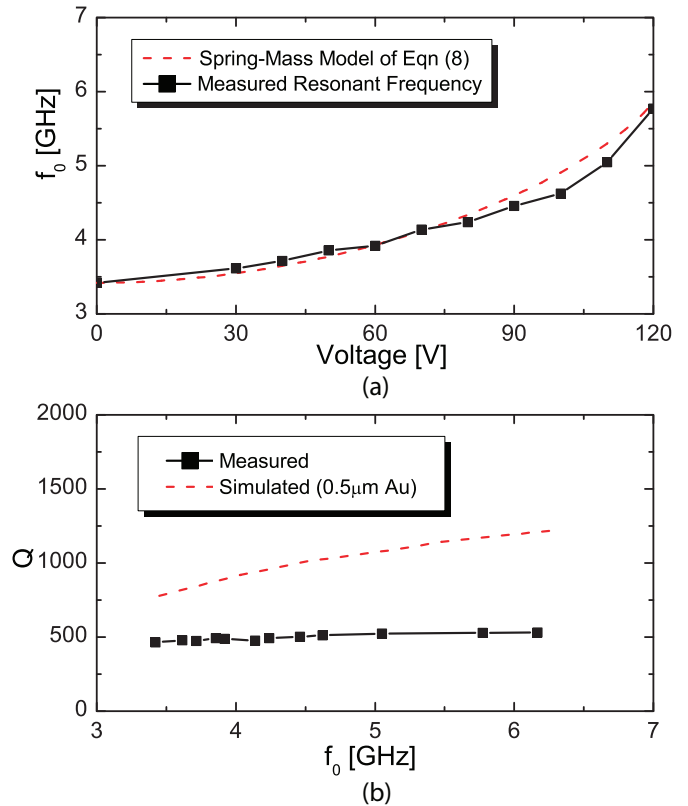


Fig. 7. Measured performances of the tunable resonator. (a) Frequency Tunability; (b) Quality Factor.

## ACKNOWLEDGEMENT

This project has been supported by the DARPA Analog Spectral Processors project. The authors are also grateful to Hjalti Sigmarsson, Himanshu Joshi and Praveen Saxena for helpful discussions and technical assistance.

## REFERENCES

- [1] L. P. B. Katehi, "Tunable Evanescent Mode Filters", *DARPA Project Report*, December 2000.
- [2] X. Gong, A. Margomenos, B. Liu, S. Hajela, L. P. B. Katehi and W. J. Chappell, "Precision Fabrication Techniques and Analysis on High-Q Evanescent-Mode Resonators and Filters of Different Geometries," *IEEE Trans. Microwave Theory & Tech.*, vol. 52, no. 11, pp. 2557-2566, November 2004.
- [3] T. A. Schwarz, and L. P. B. Katehi, "A Micromachined Evanescent Mode Resonator", *1999 European Microwave Conference Dig.*, vol. 2, pp. 403-406, October 1999.
- [4] S. M. Hou, J. H. Lang, A. H. Slocum, A. C. Weber, and J. R. White, "A High-Q Widely Tunable Gigahertz Electromagnetic Cavity Resonator", *J. Microelectromech. Syst.*, vol. 15, no. 6, pp. 1540-1545, December 2006.
- [5] H. Joshi, H. H. Sigmarsson, D. Peroulis, and W. J. Chappell, "Highly Loaded Evanescent Cavities for Widely Tunable High-Q Filters", *2007 IEEE MTT-S Int. Microwave Symp. Dig.*, pp. 2133-2136, June 2007.
- [6] R.G. Carter, J. Feng, and U. Becker, "Calculation of the Properties of Reentrant Cylindrical Cavity Resonators", *IEEE Trans. Microwave Theory & Tech.*, vol. 55, no. 12, pp. 2531-2538, December 2007.
- [7] G.M. Rebeiz, *RF MEMS, Theory, Design and Technology*, New York: J. Wiley & Sons, 2003.
- [8] High Frequency Structural Solver, Ansoft Cooperation. <http://www.ansoft.com/products/hf/hfss/>